

GPS measurements of crustal deformation within the Pacific–Australia plate boundary zone in Irian Jaya, Indonesia

S.S.O. Puntodewo ^a, R. McCaffrey ^{b,*}, E. Calais ^c, Y. Bock ^c, J. Rais ^a, C. Subarya ^a,
R. Poewariardi ^a, C. Stevens ^b, J. Genrich ^c, Fauzi ^b, P. Zwick ^b, S. Wdowski ^c

^a National Coordination Agency for Surveying and Mapping, Cibinong, Java, Indonesia

^b Department of Earth and Environmental Sciences, Rensselaer Polytechnic Institute, Troy, NY 12180-3590, USA

^c Institute of Geophysics and Planetary Physics, Scripps Institution of Oceanography, La Jolla, CA, USA

Received 15 June 1993; revised version accepted 20 June 1994

Abstract

Global Positioning System (GPS) measurements made in 1991, 1992 and 1993 provide preliminary estimates of slip distribution between the Australian and Pacific plates in Irian Jaya, Indonesia. We interpret the GPS results with constraints from earthquake mechanisms and slip vectors, recent marine surveys, and geology. Three GPS sites in southeastern Irian Jaya show motions that are within 10 mm/yr of the expected motion of Australia. A coast-to-coast N–S baseline along 140.5°E crosses all known onland regions of active deformation but reveals no more than 15 mm/yr of shortening and 20 mm/yr of left-lateral shear in the 27-month period. The remaining 40 mm/yr of expected convergence between the Pacific and Australian plates probably occurs at the New Guinea trough. GPS sites on the island of Biak, at 136°E, and at Sorong, near the western tip of Bird's Head (at 131°E), both move 90–100 mm/yr in a WSW direction relative to Irian Jaya, but less than 15 mm/yr relative to each other. These sites are on either side of the Sorong fault and demonstrate that it is not presently the major boundary between the Australian and Pacific plates. Instead the plate boundary is now south of the Sorong and Biak sites. Earthquakes suggest possible structures that accommodate motion between Bird's Head and Australia but the relative importance of them remains uncertain.

1. Introduction

Eastern Indonesia is a region of broad deformation between the Australian, Southeast Asian, Philippine Sea and Pacific plates. Within the Irian Jaya province of Indonesia (western half of New Guinea) convergence between Australia and

the Pacific is thought to be accommodated by thrusting in the Highlands and Mamberambo thrust belts (Dewey and Bird, 1970; Dow and Sukamto, 1984a; Abers, 1989) and by strike-slip motion along the Sorong–Yapen fault and faults within the Highlands thrust belt (Abers and McCaffrey, 1988). Seismicity shows that the deformation is distributed over a 400–500-km-wide zone between the southern edge of the Highlands thrust belt and the New Guinea trough in the north (Fig. 1).

* Corresponding author.

Relative motion between the Pacific and Australian plates is constrained largely from closure of the Pacific–Antarctic–Australian plate circuit as there are no reliable observations from the Pacific–Australian boundary itself (DeMets et al., 1990). In order to constrain plate motions and crustal deformation within the Pacific–Australian

plate boundary zone in Irian Jaya, we established a geodetic network with the Global Positioning System (GPS) (Fig. 1). In May 1991, a six-station network was established and occupied and these sites were occupied again in June 1992 and August 1993. This paper presents the displacements revealed by the three sets of GPS measurements

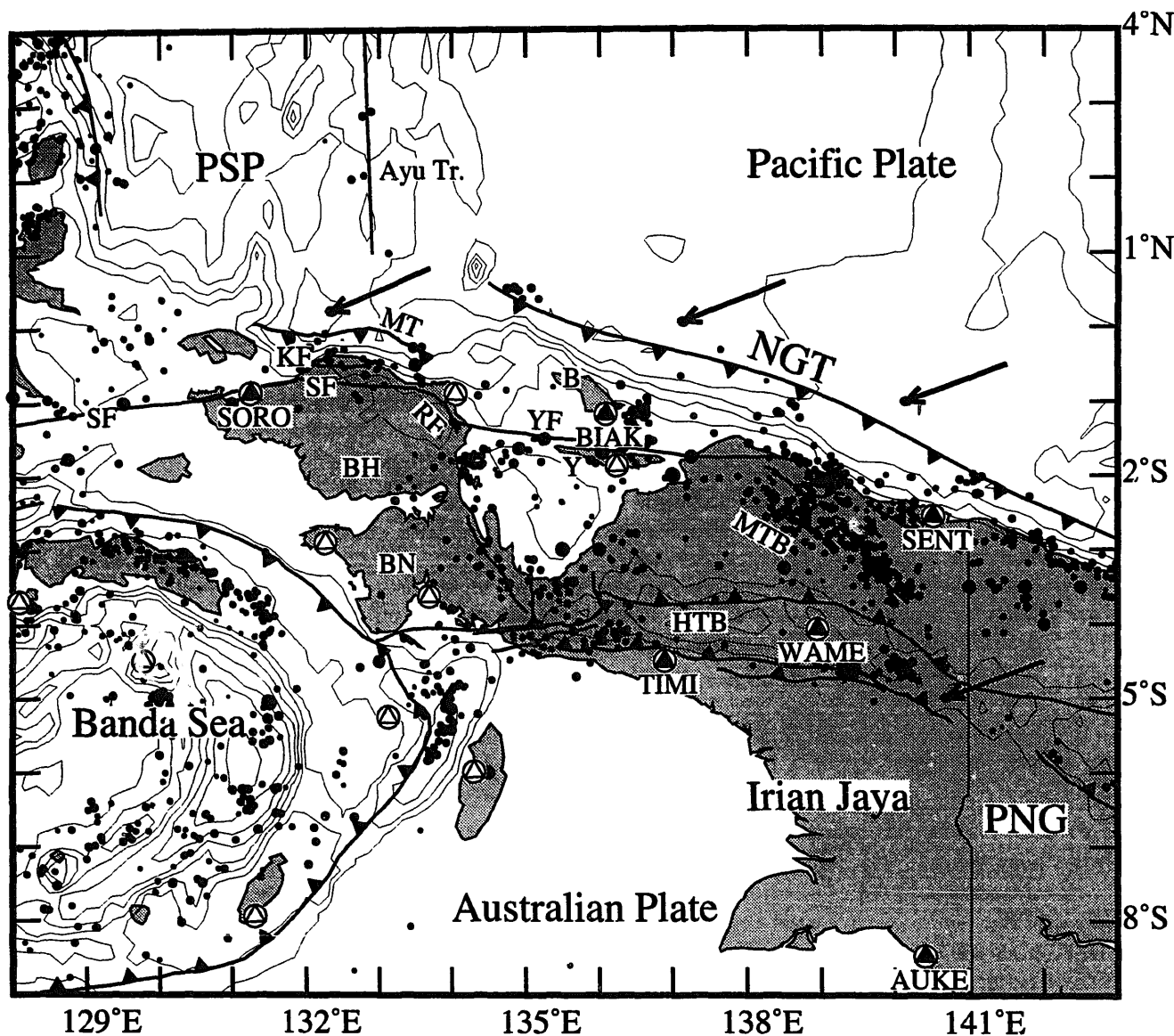


Fig. 1. Tectonic map of Irian Jaya region and GPS network. Earthquake epicenters (small dots) are from the ISC catalog for 1964–1988 and depths less than 50 km. Larger dots show earthquakes of magnitude ≥ 7 from the Pacheco and Sykes (1993) catalog. Filled triangles = GPS sites occupied in 1991, 1992 and 1993; open triangles = GPS sites occupied only in 1992 or in 1992 and 1993. Arrows show motion of Pacific plate relative to Australia. Bathymetric contours are 1000 m. PSP = Philippine Sea plate; PNG = Papua New Guinea; MT = Manokwari trough; KF = Koor fault; SF = Sorong fault; RF = Ransiki fault; NGT = New Guinea trench; Y = Yapen Island; B = Biak Island; YF = Yapen fault; BH = Bird's Head; BN = Bird's Neck; HTB = Highlands thrust belt; MTB = Mamberambo thrust belt.

at these six sites and interpretations of deformation in the Australia–Pacific plate boundary.

2. New Guinea tectonics

The island of New Guinea is the site of oblique convergence between oceanic plates and the margin of continental Australia (Fig. 1). Most convergence appears to be accommodated by crustal thickening in the onland regions instead of by subduction. The mountainous Highlands thrust belt reaches 4922 m elevation in central Irian Jaya (Fig. 1) and is bounded to the south by a foreland basin and to the north by the Mamberambo Basin, both near sea level. Crustal shortening started at the end of the Miocene (Dow and Sukanto, 1984a) and is thought to be still active, evident in recent uplift of the Highlands belt (Hamilton, 1979; Dow and Sukanto, 1984b).

Motion of the Pacific plate relative to Australia is predicted by NUVEL-1 (DeMets et al., 1990) to be at an azimuth of 248° and rate of 110 mm/yr across Irian Jaya (Fig. 1). It has been suggested that the Caroline plate is distinct from the Pacific plate and abuts Irian Jaya at the New Guinea trench. Adding the reported Caroline–Pacific rotation pole of Weissel and Anderson (1978) and the NUVEL-1 Pacific–Australia pole (DeMets et al., 1990) predicts that the motion of the Caroline plate relative to Australia is 10 to 20 mm/yr slower and about 10° more southerly than the Pacific relative to Australia. Because the existence of a separate Caroline plate is unproven and because the impact of its existence on predicted convergence across Irian Jaya is small, we will use Pacific–Australia convergence as the basis for comparison. The apparent boundary between the Pacific and Philippine Sea plates, the Ayu trough, is north of Bird's Head (Fig. 1) and indicates that the western end of the Manokwari trough accommodates subduction of the Philippine Sea plate. The sense of motion across the Ayu trough is poorly constrained but the rate is probably low (Weissel and Anderson, 1978), so that the motion of the Philippine Sea relative to Bird's Head is similar to the Pacific–Bird's Head motion. For simplicity and for lack of better

constraints we will consider the oceanic lithosphere north of Irian Jaya as part of the Pacific plate.

Topography and geologic structures of Irian Jaya trend roughly $N100^\circ E$. The Pacific–Australia relative plate motion vector is 30° away from this trend and comprises approximately 95 mm/yr of left-lateral shear parallel to structure and 55 mm/yr of shortening across the island. From summation of earthquake seismic moments and from crustal thickening estimates, apparently only 5–20% of the convergence component is accommodated within the Highlands thrust belt (Abers and McCaffrey, 1988). About 30% could be occurring in the Mamberambo thrust belt (Fig. 1) if the large thrust earthquakes there are related to crustal shortening (Abers, 1989). These earthquakes could as well be due to thrusting of the Pacific plate beneath Irian Jaya although no island arc is present near the north coast. The strike-slip component is thought to be accommodated entirely by the Sorong–Yapen and related faults near the north coast and lesser strike-slip faults within the Highlands (Abers and McCaffrey, 1988; McCaffrey and Abers, 1991).

The New Guinea and Manokwari troughs (Milsom et al., 1992) are two linear but disconnected seafloor depressions running parallel to the north coast of Irian Jaya (Fig. 1). The New Guinea trough appears to be inactive in a seismic profile near $134.5^\circ W$, where it abuts the Mapia Ridge, and does not extend topographically west of that point (Milsom et al., 1992). However, Hamilton (1979) shows a seismic profile to the east near $142.8^\circ E$ that suggests that the New Guinea trough accommodates active southward subduction. We know of no seismic profiles between 134 and $142^\circ E$. The active Manokwari trough is dominated by strike-slip motion in its western part and compression in its eastern part (Milsom et al., 1992).

3. GPS observations and data analysis

In May 1991, we established six sites in Irian Jaya (Fig. 1) and surveyed them with Trimble 4000 SST GPS receivers for 12 hours during 4

consecutive days. In June 1992, we reoccupied the six sites during a survey that spanned the entire Indonesian archipelago (Stevens et al., 1993) using Trimble 4000 SST receivers and P-code Ashtech LX-II3 receivers. The daily observation times were increased to two 8-hour sessions per day to take advantage of the expanded satellite constellation. In August 1993 the network was occupied with P-code Ashtech LX-II3 receivers and 23 hour per day observations.

GPS data were analyzed using the GAMIT/GLOBK software (King and Bock, 1992; Herring, 1992). We used data from a global network of GPS tracking stations to improve satellite orbits and to estimate Irian Jaya station positions and velocities with respect to a global terrestrial reference frame (e.g., Bock et al., 1993a). We computed an independent adjustment for each day using all data collected from 0–24 h UTC. Station positions, satellite state vectors, tropospheric zenith delay parameters and phase ambiguities were estimated from doubly differenced phase measurements (Dong and Bock, 1989; Shimada and Bock, 1992). The adjustment vector and its corresponding variance–covariance matrix for station positions and satellite orbital elements for each day were then passed to a Kalman filter (Herring et al., 1990; Feigl et al., 1993) to estimate station positions and velocities for the Irian Jaya sites. For the 1991 analysis we used all available global tracking data and the Irian Jaya data in independent daily solutions. In 1992 and 1993, we used the daily global solutions computed at Scripps Institution of Oceanography in support of the Permanent GPS Geodetic Array (PGGA) in southern California and the International GPS Service for Geodynamics (IGS) (Beutler and Brockman, 1993; Bock et al., 1993b). We analyzed data from tracking sites around the Pacific Rim that provided mutual satellite visibility with the Irian sites. All five sets of daily solutions, the 1991 global/Irian Jaya set, the 1992 and 1993 IGS/PGGA set and the 1992 and 1993 Irian Jaya/Pacific Rim set were used in the GLOBK Kalman filter to estimate station positions and velocities for the Irian Jaya sites. All computations were performed while tightly constraining the coordinates of a subset of the global tracking

coordinates in the International Terrestrial Reference Frame 1992 (ITRF92) (Altamimi and Boucher, pers. commun., 1993). This reference frame also includes velocities of the global tracking sites. The ITRF92 site velocities are based on the no-net-rotation (NNR) NUVEL-1 plate motion reference frame (DeMets et al., 1990; Argus and Gordon, 1991) and adjusted to satisfy global very long baseline interferometry and satellite laser ranging data where available. The adjusted tracking site velocities differ by no more than 10 mm/yr from their NNR velocities. The coordinates and velocities of the Irian Jaya sites are calculated in the ITRF92 frame and, due to the similarity of the ITRF92 and NNR tracking site velocities, we will compare calculated GPS velocities (in the ITRF92 frame) to predicted NNR velocities.

4. GPS results and tectonic interpretations

Velocities of the Irian Jaya GPS sites in the ITRF92 reference frame are shown in Table 1 and Fig. 2a. GPS vectors for Merauke (AUKE), Timika (TIMI), Wamena (WAME) and Sentani (SENT) show motions in general agreement with those of the Australian plate in the NNR reference frame. GPS vectors at Biak (BIAK) and Sorong (SORO) are more similar to the Pacific than to the Australian plate.

The AUKE and TIMI sites, south of the Irian Jaya thrust belt, are likely on the Australian plate. These two sites and WAME have GPS vectors that are within 8 mm/yr in northern and eastern components of the motion of Australia in the NNR reference frame. Velocities of the Irian Jaya GPS sites relative to Australia produced by subtracting the predicted NNR motion of Australia from each site, are displayed in Fig. 2b. With this definition of the Australian reference frame, the AUKE, TIMI and WAME sites show no significant motion. The SENT site moves slowly to the southwest at about 25 mm/yr and SORO and BIAK move about 100 mm/yr west-southwest relative to Australia. The observed motions of the GPS sites relative to the Pacific plate and the expected motions assuming they are on

the Australian plate, are shown in Fig. 2c. From these plots we see that the BIAK and SORO sites move at a few centimeters per year relative to the Pacific and more rapidly relative to Australia.

We calculated a pole of rotation for the southeastern part of Irian in the NNR frame constrained by the GPS vectors at the WAME, TIMI and AUKE sites. The resulting pole, at 30.0°N, 57.4°E, and angular rotation rate of 0.69°/Ma, gives a weighted RMS misfit to the velocities of 1.8 mm/yr (the individual misfits are the velocities of WAME, TIMI and AUKE relative to southeastern Irian in Table 1). The Australia–NNR pole (33.8°N, 33.2°E, and angular rotation rate of 0.68°/Ma; Argus and Gordon, 1991) gives a weighted misfit RMS of only 3.0 mm/yr, indicating that Irian is likely part of the Australian plate. GPS vectors relative to the southeastern Irian block (in the reference frame defined by the WAME, TIMI and AUKE sites) are shown in Fig. 2d and Table 1. SENT moves about 25 mm/yr to the west-southwest and BIAK and SORO move 85 to 100 mm/yr at 255° azimuth relative to southeastern Irian (Fig. 2d).

We also calculated seismic strain rates and average slip directions for five regions of Irian Jaya using published earthquake fault plane solu-

tions (Table 2; Fig. 3). The moment tensors for all earthquakes in a specified geographic volume are summed and from this sum the strain rates and the relative velocities of the boundaries of the volume are derived. The method is from Kostrov (1974) and a detailed description along with its weaknesses is given by Jackson and McKenzie (1988). Such calculations for Irian Jaya were done by Abers (1989) using earthquake data from 1963 through 1987; here we extend the data set through 1993. We also calculated the average slip vector for each region by estimating a double couple from the moment tensor sum (Table 2).

4.1. Deformation across the New Guinea thrust belt and the Mamberambo Basin

The coast-to-coast N–S baseline from SENT to AUKE crosses the known active thrust belts of Irian Jaya. Our GPS results are consistent with some left-lateral shear on E–W planes between these two sites but the compressional deformation rate across the Highlands thrust belt and the Mamberambo thrust belt is less than 15 mm/yr, much smaller than the 55 mm/yr convergence required to accommodate Pacific–Australia motion.

The largest earthquakes in Irian Jaya are found

Table 1
Velocities and standard errors (mm/yr) of Irian Jaya sites from comparison of 1991 to 1993 GPS results

Site	Latitude (°S)	Longitude (°E)	V_n	σ_n	V_e	σ_e	V	σ_v	Azimuth (°)
<i>Relative to NNR</i>									
SENT	–2.56	140.52	55.1	5.0	16.5	15.5	57.5	16.5	17
AUKE	–8.47	140.41	66.8	4.2	37.3	13.0	76.5	13.8	29
WAME	–4.07	138.95	65.6	5.0	32.7	15.0	73.3	15.8	26
TIMI	–4.50	136.90	65.6	4.2	45.2	13.0	79.7	13.8	35
SORO	–0.87	131.25	39.3	5.0	–59.8	18.0	71.6	18.7	303
BIAK	–1.16	136.09	43.0	5.0	–46.5	15.0	63.3	15.8	313
<i>Relative to southeastern Irian Jaya</i>									
SENT	–2.56	140.52	–10.9	5.0	–22.2	15.7	24.7	16.5	244
AUKE	–8.47	140.41	0.8	4.2	–1.8	13.2	2.0	13.8	295
WAME	–4.07	138.95	–0.1	5.0	–6.3	15.0	6.3	15.8	269
TIMI	–4.50	136.90	0.3	4.2	6.0	13.2	6.0	13.8	87
SORO	–0.87	131.25	–24.5	5.0	–98.4	18.2	101.4	18.7	256
BIAK	–1.16	136.09	–22.2	5.0	–85.1	15.0	87.9	15.8	255

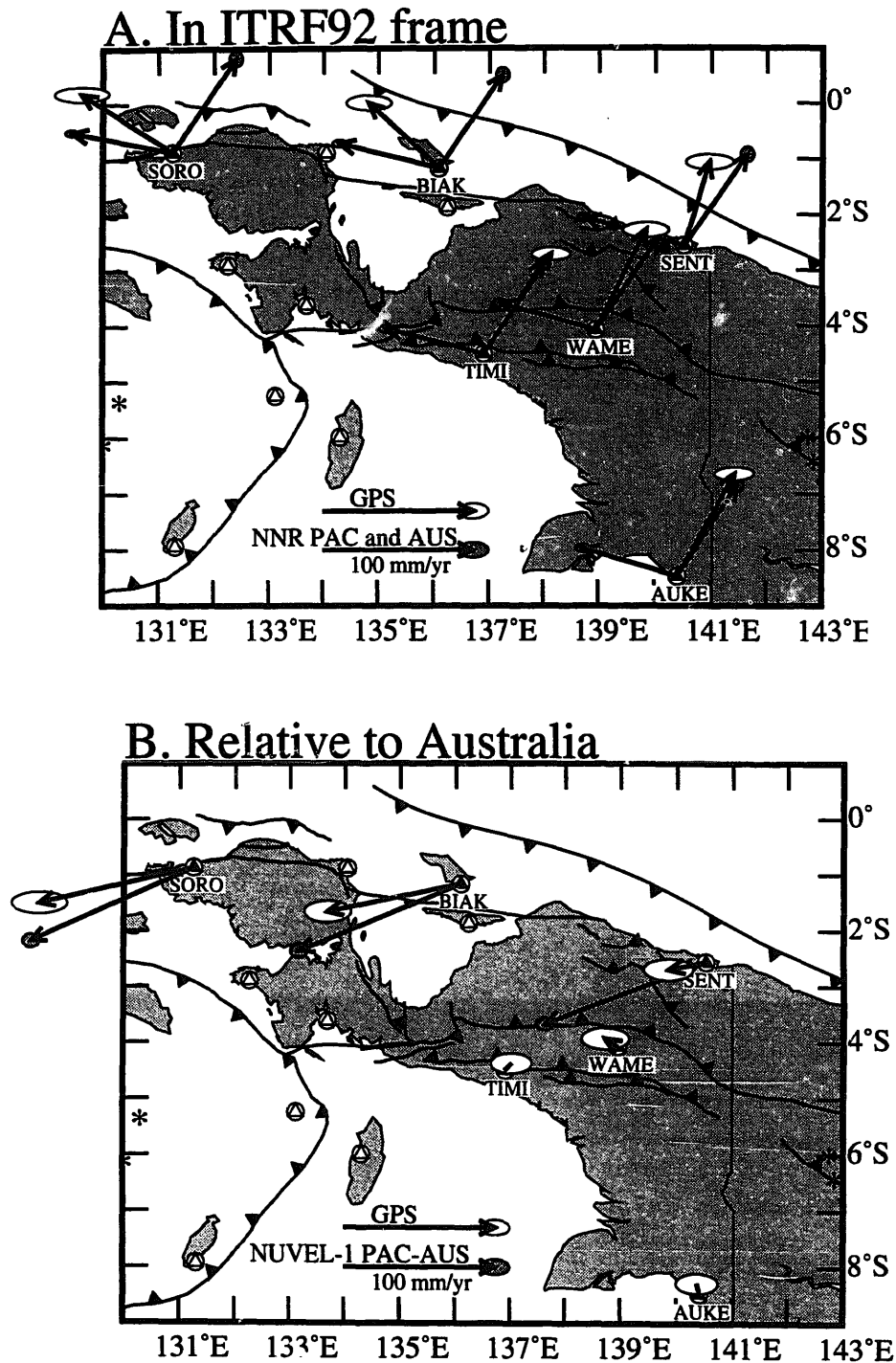
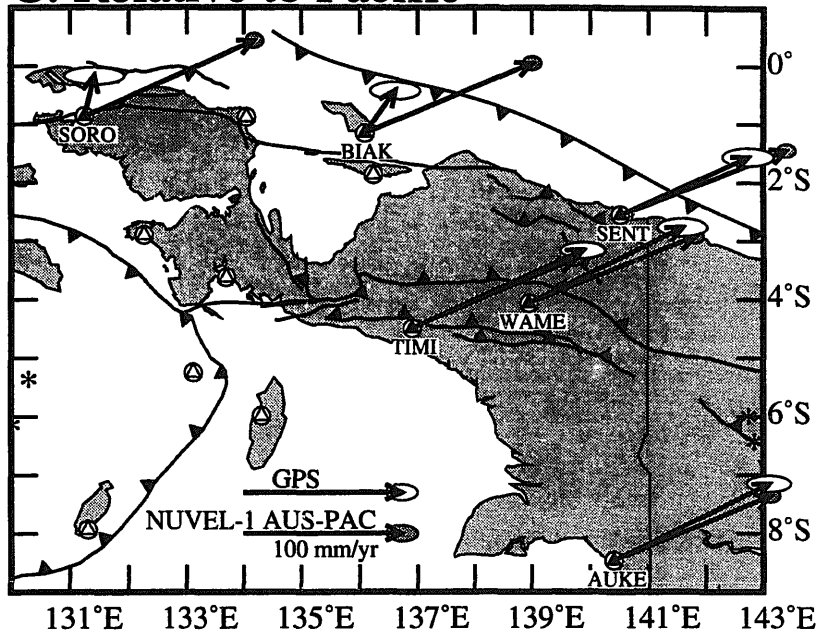


Fig. 2. (a) *GPS* velocity vectors and standard error ellipses for 1991–1993 in the International Terrestrial Reference Frame 1992 (ITRF92). *GPS* vectors are those with lighter shading in error ellipse. The ITRF92 is similar to the no-net-rotation (NNR)–NUVEL-1 reference frame (Argus and Gordon, 1991), as discussed in text. Also shown are predicted Australia–NNR vectors (the NE-trending vectors) and predicted Pacific–NNR vectors (the westerly-trending vectors). (b) *GPS* vectors relative to Australia (the predicted Australia–NNR vector is subtracted from the *GPS* NNR vector at each site). Also shown are the predicted vectors of the Pacific plate relative to Australia at the *SORO*, *BIAK* and *SENT* sites. (c) *GPS* velocity vectors relative to Pacific plate (the predicted Pacific–NNR vector is subtracted from the *GPS* NNR vector at each site). Also shown are the predicted vectors of the Australian plate relative to the Pacific. (d) *GPS* velocity vectors relative to a rigid southeastern Irian block (defined by the *WAME*, *TIMI* and *AUKE* sites).

beneath the Mamberambo thrust belt and typically show thrusting with NE-trending slip vectors (Fig. 3). Abers (1989) estimated rates of 24 mm/yr

of N–S shortening and 23 mm/yr of shear, presumably left lateral on an E–W plane, by summing seismic moments of earthquakes beneath

C. Relative to Pacific



D. Relative to SE Irian

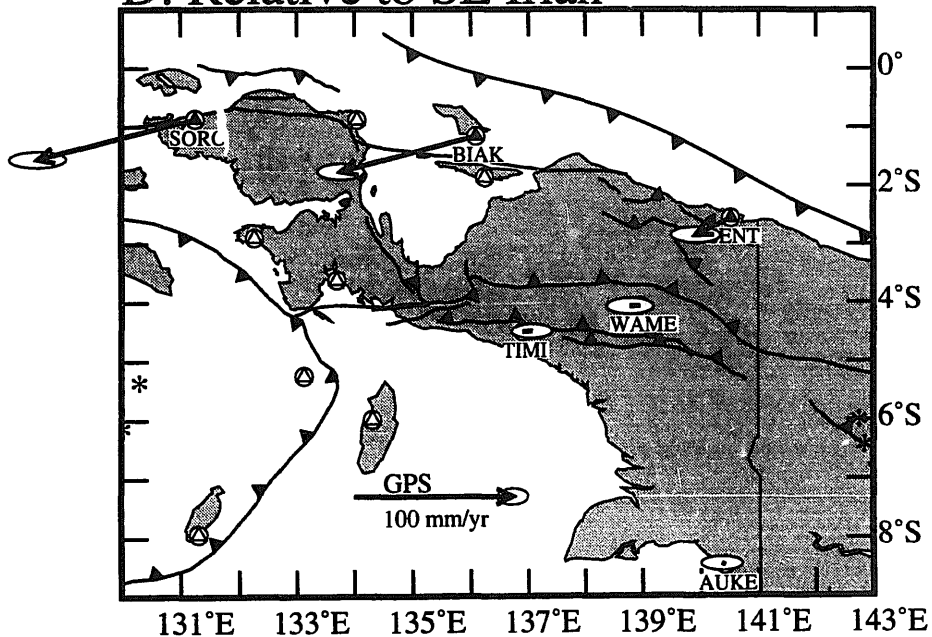


Fig. 2 (continued).

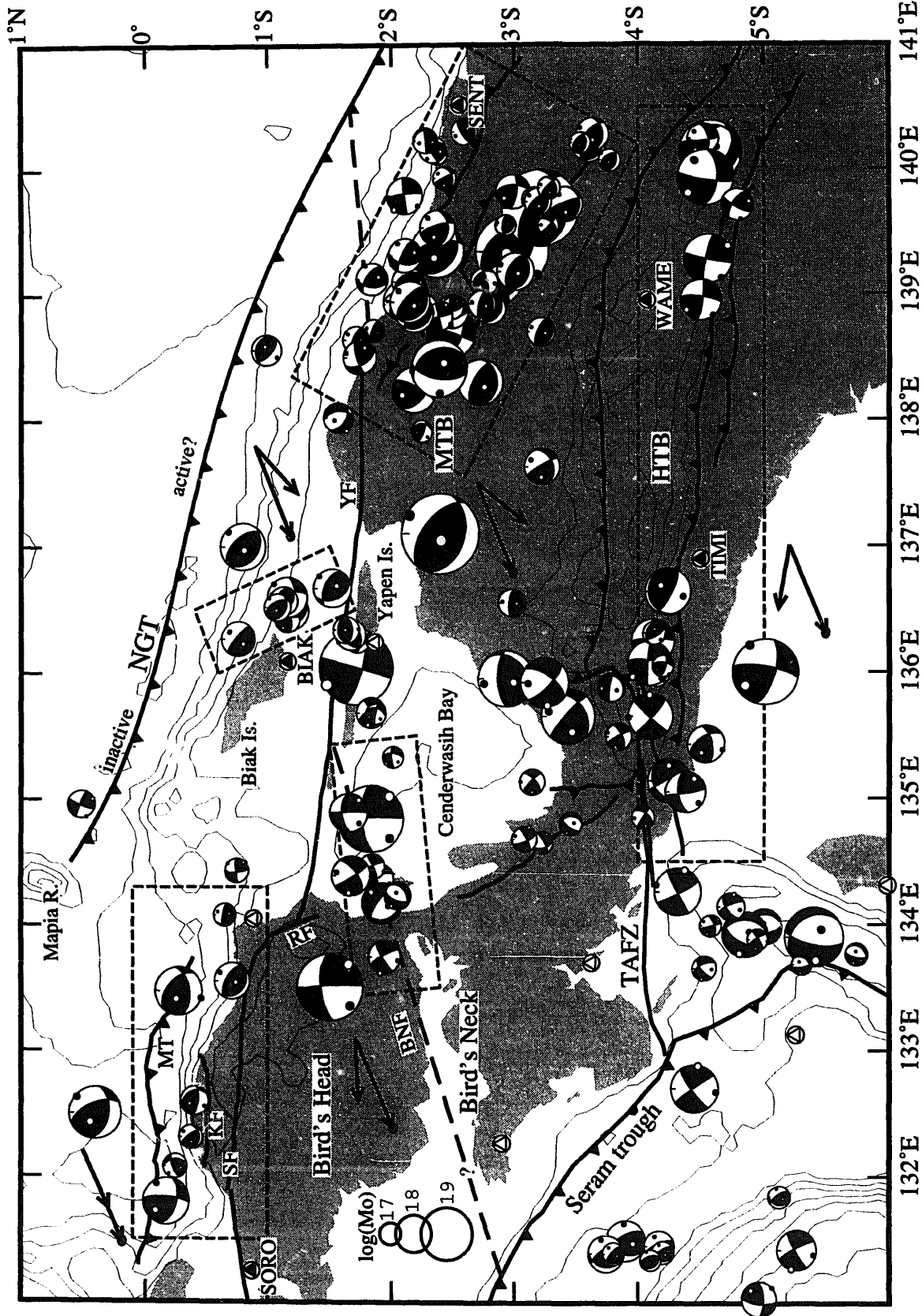


Fig. 3. Tectonic map of Irian Jaya showing fault plane solutions, faults (solid lines) and inferred faults (dashed lines). Fault plane solutions with shaded quadrants are from Harvard centroid-moment tensor catalog (1977–1993) and from Abers (1989). Those with black quadrants are the double couples derived from the moment tensor sum of all events within the nearby boxes enclosed by dashed lines. Size of focal sphere is scaled to log of seismic moment (scale shown at left). Long arrows near each enclosed region show expected motion of the Pacific relative to Australia and the short arrows show slip vector azimuths derived from summing moment tensors of earthquakes within the boxes (Table 2). Slip vectors are taken for the S-dipping planes in the Manokwari, Biak and Mamberambo regions, and for the easterly-striking planes in the Bird's Neck and Highlands thrust belt regions. Bathymetry and topography are contoured at 1000 m intervals. *MT* = Manokwari trough; *KF* = Koor fault; *SF* = Sorong fault; *BNF* = Bird's Neck fault; *RF* = Ransiki fault; *NGT* = New Guinea trench; *YF* = Yapen fault; *TAFZ* = Tarera–Aiduna fault zone; *HTB* = Highlands thrust belt; *MTB* = Mamberambo thrust belt.

the Mamberambo Basin and the Highlands. We recalculated these rates using earthquakes spanning a longer time period (31 years) and get somewhat lower numbers (Table 2). The GPS vector of SENT relative to southeastern Irian (25 mm/yr) is similar in magnitude to our estimate of 22 mm/yr of shortening across the Mamberambo Basin. The S-dipping nodal planes of thrust earthquakes in the Mamberambo thrust zone project to the surface near the north coast (north of

the SENT site); hence the SENT site may be within the deforming zone and shows only part of the total shortening. The WAME site, north of the Highlands thrust belt but south of the Mamberambo thrust zone, did not appear to move significantly relative to AUKE and TIMI, which is consistent with the seismic slip rates in the Highlands thrust belt (Table 2); < 1 mm/yr of N–S shortening and < 10 mm/yr of left-lateral E–W shear. It appears then from both geodetic

Table 2
Results of summing moment tensors for regions shown in Fig. 3

a. Moment tensor sums by region ($\times 10^{16}$ Nm)									
Region	<i>N</i>	<i>X</i> -axis azimuth	ΣM_0	ΣM_{XX}	ΣM_{XY}	ΣM_{XZ}	ΣM_{YY}	ΣM_{YZ}	ΣM_{ZZ}
Biak	7	N45°E	481	-412	15	-169	116	-17	297
Manokwari Tr.	7	North	1086	-471	-533	124	-157	-458	628
Bird's Neck	10	N5°W	8339	630	-7337	448	-59	3126	-571
Highlands	24	North	9603	2150	-5265	2190	-2972	-2225	823
Mamberambo	49	N30°E	69498	-55891	2382	-17866	171	-11188	55720

b. Summary by region									
Region	L_x (km)	L_y (km)	L_z (km)	Moment, (10^{18} Nm)	Strike (°)	Dip (°)	Rake (°)	Slip vector	
Biak	70	130	30	4.06	127	33	80	228	
Manokwari Tr.	100	310	30	9.11	99	47	43	246	
Bird's Neck	80	200	20	80.1	265	67	355	267	
Highlands	100	650	20	66.7	106	67	15	280	
Mamberambo	150	300	30	597.0	107	37	72	219	

c. Strain rates by region ($\times 10^{-9}$ /yr)							
Region	$\dot{\epsilon}_{XX}$	$\dot{\epsilon}_{XY}$	$\dot{\epsilon}_{XZ}$	$\dot{\epsilon}_{YY}$	$\dot{\epsilon}_{YZ}$	$\dot{\epsilon}_{ZZ}$	
Biak	-5.4	0.2	-2.2	1.5	-0.2	3.9	
Manokwari Tr.	-1.8	-2.1	0.5	-0.6	-1.8	2.4	
Bird's Neck	7.1	-82.6	5.0	-0.7	35.2	-6.4	
Highlands	6.0	-14.6	6.1	-8.2	-6.2	2.3	
Mamberambo	-149.1	6.4	-47.6	0.5	-29.8	148.6	

d. Velocities by region (in mm /yr)									
Region	V_{XX}	V_{XY}	V_{XZ}	V_{YX}	V_{YY}	V_{YZ}	V_{ZX}	V_{ZY}	V_{ZZ}
Biak	-0.4	0.0	-0.1	0.0	0.2	-0.0	-0.2	-0.0	0.1
Manokwari Tr.	-0.2	-0.6	0.0	-0.2	-0.2	-0.1	0.0	-0.5	0.1
Bird's Neck	0.6	-16.5	0.1	-6.6	-0.1	0.7	0.4	7.0	-0.1
Highlands	0.6	-9.5	0.1	-1.5	-5.4	-0.1	0.6	-4.0	0.0
Mamberambo	-22.4	1.9	-1.4	1.0	0.1	-0.9	-7.1	-9.0	4.5

N is the number of earthquakes in each region. The sums are over a 31-year time period (1963–1993). The *X*-axis is positive in the direction given, *Y* is positive in the direction 90° clockwise from *X*, and *Z* is positive down. L_x , L_y and L_z are dimensions of regions in kilometers. Positive normal strains and velocities are extensional and positive shear strains and velocities are right lateral. $\dot{\epsilon}_{ij} = \Sigma M_{ij} / \mu V t$, where μ is the shear modulus (4.5×10^{10} N/m²), V is the volume of the region ($V = L_x L_y L_z$) and t is time (Kostrov, 1974). The velocities $V_{ij} = \dot{\epsilon}_{ij} L_i$.

and seismological data that most of the shortening beneath the onland part of Irian Jaya now occurs in the Mamberambo thrust belt but that it is not enough to accommodate convergence between the Pacific and Australia.

4.2. *The Sorong–Yapen and Koor faults*

Despite the prevailing notion that the Sorong–Yapen fault forms the main boundary between the Pacific and Australian plates in northern Irian Jaya, very little is known about this fault system. East of Bird's Head and south of Biak Island, the Yapen fault is active seismically, producing occasional large left-lateral strike-slip earthquakes (Fig. 3). The Yapen fault probably forms the strait between Biak and Yapen islands and may comprise more than one strand (Hamilton, 1979). To the east, the fault comes back onto land but is not distinct and either merges with the Mamberambo thrust belt or extends out to the New Guinea trough. West of Biak, the Sorong fault can be seen in the northern part of Bird's Head. It offsets streams by only 300 m or so (Dow and Sukanto, 1984a) and the eastern end is truncated by the NW-trending Ransiki fault (Fig. 3). This part of the fault system is displaced 40 km to the north relative to the Yapen fault. Nevertheless, Dow and Sukanto (1984a) suggest that there has been at least 370 km of left-lateral slip on the Sorong–Yapen fault since the Middle Miocene. Hamilton (1979) suggests that the broad strand of the fault mapped by Visser and Hermes (1962) extending east-northeast from the town of Sorong (near site SORO) is probably an old melange belt rather than a young shear zone. If so, the Sorong fault goes offshore to the west of Bird's Head several kilometers north of the SORO GPS site. The western end of the Manokwari trough may connect with the Sorong fault west of Bird's Head through a fault in the strait north of the SORO site (J. Milsom, pers. commun., 1993). About 40 km north of the Sorong fault and 20 km south of the north coast of Bird's Head is the Koor fault, which presently separates continental rocks from oceanic rocks (Dow et al., 1986). Earthquakes of $M \geq 7$ in this century are located near the north

coast of Bird's Head rather than near the mapped trace of the Sorong fault (Everingham, 1974). The mechanisms of these earthquakes are unknown and they may have occurred either on the Koor fault or at the Manokwari trough.

The BIAK site moves at 88 ± 16 mm/yr while the SORO site moves 101 ± 19 mm/yr, both at azimuths of 255° relative to southeastern Irian (Fig. 2d). These vectors can account for a large part of the motion between Pacific and Australia, predicted by NUVEL-1 to be 116 mm/yr at azimuth 247° . The N–S component is only about one-half of the expected convergence rate at both sites. Nevertheless, the main plate boundary must be south of these sites.

GPS vectors indicate that SORO moves less than 20 mm/yr west relative to BIAK, which is the opposite sense of slip expected if the Sorong or Koor fault or both are active left-lateral faults (BIAK is well north of and SORO is at least 15 km south of the Sorong fault; Fig. 3). While the uncertainties in these vectors are somewhat large and deformations near faults can be complex, we can rule out left-lateral shear at rates of tens of millimeters per year between these two sites, and suggest that the Sorong and Koor faults, at least where they are seen on Bird's Head, are now inactive. If either of these faults were slipping rapidly then the slip vectors of earthquakes at the Manokwari trough would be rotated away from the convergence direction and be more perpendicular to the trench (McCaffrey, 1992). However, the average slip vector at the Manokwari trough is parallel to the Pacific–Australia vector, suggesting also that the Sorong and Koor faults are not slipping rapidly.

4.3. *The New Guinea and Manokwari troughs*

Subtracting the NNR–Pacific vector from the BIAK GPS vector (Fig. 2c) indicates that Biak Island and the Pacific plate converge in a 216° azimuth at a rate of about 33 mm/yr. Slip vectors of thrust earthquakes near Biak Island show a similar convergence azimuth of 228° (Table 2; Fig. 3). Thus, at the longitude of Biak Island, about 30 mm/yr of convergence probably occurs on the New Guinea trough or other thrust faults

near Biak Island. Note that the seismic profile that shows inactivity at the New Guinea trough (Milsom et al., 1992) is west of Biak Island, near 134.6°E. Since our GPS results indicate less than 15 mm/yr of shortening across the Mamberambo thrust belt and the Highlands thrust belt, we expect that the New Guinea trough is active from about the longitude of Biak to the east and accommodates at least 30 mm/yr convergence. Some of the thrust earthquakes beneath the Mamberambo basin (Fig. 3) might be related to the New Guinea trough rather than to convergence within the thrust belt.

The Manokwari trough north of Bird's Head is part of an active fault zone accommodating thrusting of the oceanic floor beneath Bird's Head (Milsom et al., 1992). The motion expected across the Manokwari trough and the Sorong and Koor faults is shown by the SORO site relative to the Pacific (Fig. 2c) which is 26 mm/yr at 13° azimuth. This motion is nearly perpendicular to the E–W-trending trench. However, Milsom et al. (1992) note evidence for a large amount of shear in the sonar imagery of the upper plate south of the Manokwari trough and slip vectors of earthquakes at the Manokwari trough are parallel to the Pacific–Australia convergence vector (Table 2; Fig. 3), highly oblique to the trench. Summing of the seismic moments of earthquakes at the Manokwari trough and Sorong fault gives a slip rate of about 1 mm/yr consisting almost entirely of shearing (Table 2), which is considerably less than the total expected rate of 26 mm/yr inferred from GPS but similar to the expected component of E–W shear (6 mm/yr). To make up the missing seismic slip on the Manokwari trough would require a thrust earthquake of moment magnitude of at least 7.7 (assuming 30 years at 25 mm/yr, fault length of 300 km, downdip fault width of 50 km and rigidity of 4.5×10^{10} N/m²).

The western end of the active New Guinea trough (near 135–136°E) may connect by a SW-trending left-lateral transform fault or shear zone to the eastern end of the Manokwari trough around 134°E (Fig. 3). This transform is required if the New Guinea trench is active east of Biak, and one earthquake mechanism east of the north-

ern part of Bird's Head shows the correct orientation and sense of slip (Fig. 3). The Manokwari trough, rather than the Sorong fault, now forms the boundary between the Pacific plate and the Bird's Head block.

4.4. Motion of Bird's Head relative to Australia

Bird's Head (BH) of New Guinea is a large block of continental crust overlain by early Mesozoic–late Tertiary sedimentary rocks that are indistinguishable from those of the Australian continent to the south, implying that Bird's Head has been part of Australia for a long time and that the total relative motion between them has been small. Paleomagnetic data from Bird's Head (Klootwijk et al., 1987) and the island of Misool (at 2°S, 130°E; Thrupp et al., 1987), which is connected to Bird's Head, suggest little motion relative to Australia, except for a possible 30–40° rotation at some poorly constrained time in the past. The present motion of Bird's Head relative to Australia is unknown but some westward motion was suggested by McCaffrey and Abers (1991) resulting from left-lateral shear in the Highlands thrust belt.

GPS results indicate a significant WSW component of motion of Bird's Head relative to southeastern Irian. The SORO site displays motion which is close to the predicted motion of the Pacific plate and quite different from that of the Australian plate (Fig. 2). Relative to southwestern Irian it appears to move at 100 mm/yr to the west-southwest (Fig. 2d). The absence of significant motion between BIAK and SORO suggests that the slip rate on the Sorong fault is small and the SORO motion is not due to elastic strain near the Sorong fault. Therefore, the motion of SORO relative to Australia is probably largely accommodated by faults south of SORO. Earthquake activity suggests two possible places where slip between Bird's Head and Australia could occur. The first is in the Highlands thrust belt where earthquakes suggest that there could be as much as 10–20 mm/yr of left-lateral shear (Table 2; McCaffrey and Abers, 1991). The WAME to TIMI baseline shows 12 mm/yr shortening and uncertainties allow 20 mm/yr E–W convergence

between these sites, consistent with a left-lateral shear zone between them. West of the TIMI site and south of Bird's Head, the Tarera–Aiduna fault zone trends westerly toward the Banda arc (Fig. 3). This fault is visible as a linear feature on a radar image (Hamilton, 1979) and forms a topographically sharp southern boundary of Bird's Head. Its slip rate is estimated at 20 mm/yr (Hamilton, 1979; McCaffrey and Abers, 1991).

A second possible site for motion of Bird's Head relative to Australia is at the southern end of BH, called Bird's Neck, where an ENE-trending zone of earthquakes display predominantly left-lateral strike slip (Fig. 3). Summation of seismic moment tensors for the events within the box (Table 2; Fig. 3) shows 16 mm/yr of left-lateral shear on an E-trending vertical plane over the past 31 years. The average strike direction of the earthquakes (265° , Fig. 3, Table 2) and the orientation of the earthquake zone are nearly parallel to the SORO–southeastern Irian GPS vector (256°) and the Pacific–Australia vector (247°). The summed seismic slip rate on the two faults discussed above is still too low by a factor of 2 to account for all SORO–southeastern Irian motion. Hence, either the seismic slip rates are low in the time period studied or other faults take up significant motion. Another possible location for motion between Bird's Head and Australia is along the eastern shore of the Cenderwasih Bay where large earthquakes have occurred recently (Fig. 3).

5. Conclusions

Three sets of GPS measurements in the Irian Jaya province of Indonesia show that the oblique convergence between the Pacific and Australian plates is accommodated in two very different ways. At Biak Island and to the east, convergence between Australia and the Pacific is taken up partially within the Highlands and Mamberambo thrust belts but a large portion must occur at the New Guinea trough or on other S-dipping faults that crop out north of the SENT site. The E–W shear component occurs mostly south of Biak Island (perhaps largely at the Yapen fault). The

eastern end of the Yapen fault probably connects with the New Guinea trench, as suggested in Fig. 3, or may merge with the Mamberambo thrust belt. In the region east of Biak, the Pacific–Australia oblique convergence appears to be highly partitioned between thrusting at the New Guinea trench and in the Mamberambo thrust belt and strike slip at the Yapen fault and in the Highlands.

West of Biak Island (136°W), the Pacific–Australia convergence appears to be accommodated largely by rapid westward motion of Bird's Head relative to Australia and less important thrusting of the Pacific beneath the New Guinea trench and Manokwari trough. We suggest that a branch of the Yapen fault (Bird's Neck fault; BNF in Fig. 3) heads west-southwest and separates southern Bird's Head (SBH) from Bird's Neck, accounting for some of the SORO–Australia relative motion. A second branch heads westward into Bird's Head and is truncated by the Ransiki fault but may connect with the Sorong fault. The slip rate on this fault is probably low. Some thrusting occurs at the Manokwari and New Guinea trenches and may accommodate a large part of the required convergence. Other faults south of SORO are needed to take up the shear component but the distribution of this strain is not clear.

Acknowledgments

This work is part of a collaborative agreement between the Indonesian National Coordination Agency for Surveying and Mapping (BAKO-SURTANAL, Cibinong, Indonesia), Rensselaer Polytechnic Institute (Troy, NY) and Scripps Institution of Oceanography (San Diego, CA). We thank the many people who collected data, colleagues who work under the umbrella of the International GPS Service for Geodynamics (IGS) providing timely and reliable global tracking data, Martin Hendy and John Manning from AUSLIG, Paul Tregoning and Fritz Brunner from UNSW for operating GPS receivers in Australia, and Peng Fang and Keith Stark who maintain the Scripps Orbit and Permanent Array Center.

Comments by John Milsom and Robert Hall are appreciated. We thank Mike Bevis and Don Argus for reviews. Supported by the Indonesian government, NSF grants EAR-8908759 (RPI), EAR-9114349 (RPI), EAR-8817067 (SIO), EAR-9114864 (SIO), EAR-9004376 (SIO) and NASA grant NAGW-2641 (SIO).

References

- Abers, G.A., 1989. Active tectonics and seismicity of New Guinea. Ph.D. Thesis, Massachusetts Institute of Technology.
- Abers, G.A. and McCaffrey, R., 1988. Active deformation in the New Guinea fold-and-thrust belt: seismological evidence for strike-slip faulting and basement-involved thrusting. *J. Geophys. Res.*, 93: 13,332–13,354.
- Argus, D.F. and Gordon, R.G., 1991. No-net-rotation model of current plate velocities incorporating plate motion model NUVEL-1. *Geophys. Res. Lett.*, 18: 2039–2042.
- Beutler, G. and Brockman, E. (Editors), 1993. Proc. 1993 IGS Workshop, Int. Assoc. Geodesy, Univ. Bern Press, Bern.
- Bock, Y., Agnew, D.C., Fang, P., Genrich, J.F., Hager, B.H., Herring, T.A., Hudnut, K.W., King, R.W., Larsen, S., Minster, J.B., Stark, K., Wdowinski, S. and Wyatt, F.K., 1993a. Detection of crustal deformation from the Landers earthquake sequence using continuous geodetic measurements. *Nature*, 363: 337–340.
- Bock, Y., Zhang, J., Fang, P., Genrich, J.F., Stark, K. and Wdowinski, S., 1993b. One year of daily satellite orbit and polar motion estimation for near real time crustal deformation monitoring. In: I.I. Mueller and B. Kolaczek (Editors), Proc. IAU Symp., Developments in Astrometry and their Impacts on Astrophysics and Geodynamics, 156. Kluwer, Dordrecht, pp. 279–284.
- DeMets, C., Gordon, R.G., Argus, D.F. and Stein, S., 1990. Current plate motion. *Geophys. J. Int.*, 101: 425–478.
- Dewey, J.F. and Bird, J.M., 1970. Mountain belts and the new global tectonics. *J. Geophys. Res.*, 75: 2625–2647.
- Dong, D. and Bock, Y., 1989. GPS Network analysis with phase ambiguity resolution applied to crustal deformation studies in California. *J. Geophys. Res.*, 104: 3949–3966.
- Dow, D.B. and Sukamto, R., 1984a. Western Irian Jaya: the end product of oblique plate convergence in the late Tertiary. *Tectonophysics*, 106: 109–139.
- Dow, D.B. and Sukamto, R., 1984b. Late Tertiary to Quaternary tectonics of Irian Jaya. *Episodes*, 7: 3–9.
- Dow, D.B., Robinson, G.B., Hartono, U. and Ratman, N., 1986. Geologic map of Irian Jaya, Indonesia, 1:1,000,000 scale. Geol. Res. Dev. Cent. Indonesia, Bandung.
- Everingham, I.B., 1974. Large earthquakes in the New Guinea–Solomon islands area, 1873–1972. *Tectonophysics*, 23: 323–338.
- Feigl, K.L., Agnew, D.C., Bock, Y., Dong, D., Donnellan, A., Hager, B.H., Herring, T.A., Jackson, D.D., Jordan, T.H., King, R.W., Larsen, S., Larsen, K.M., Murray, M.H., Shen, Z. and Webb, F.H., 1993. Measurement of the velocity field of central and southern California, 1984–1992. *J. Geophys. Res.*, 98: 21,677–21,712.
- Hamilton, W., 1979. Tectonics of the Indonesian region. U.S. Geol. Surv., Prof. Pap., 1078: 1–345.
- Herring, T.A., 1992. Documentation for the global Kalman filter VLBI and GPS analysis program (GLOBK), Version 3.0. (unpubl.).
- Herring, T.A., Davis, J.L. and Shapiro, I.I., 1990. Geodesy by radio interferometry: the application of Kalman filtering to the analysis of very long baseline interferometry data. *J. Geophys. Res.*, 95: 12,561–12,581.
- Jackson, J. and McKenzie, D., 1988. The relationship between plate motions and seismic moment tensors, and the rates of active deformation in the Mediterranean and Middle East. *Geophys. J.*, 93: 45–73.
- King, R.W. and Bock, Y., 1992. Documentation for the GAMIT GPS analysis software, Release 9.1 (unpubl.).
- Klootwijk, C., Giddings, J., Sunata, W., Pigram, C., Loxton, C., Davies, H., Rogerson, R. and Falvey, D., 1987. Paleomagnetic constraints on terrane tectonics in New Guinea. *Pacific Rim Congr.* 87.
- Kostrov, B.V., 1974. Seismic moment and energy of earthquakes, and seismic flow of rocks. *Izv. Acad. Sci. USSR, Phys. Solid Earth*, 1: 23–40.
- McCaffrey, R., 1992. Oblique plate convergence, slip vectors, and forearc deformation. *J. Geophys. Res.*, 97: 8905–8915.
- McCaffrey, R. and Abers, G.A., 1991. Orogeny in arc-continent collision: the Banda arc and western New Guinea. *Geology*, 19: 563–566.
- Milsom, J., Masson, D., Nichols, G., Sikumbang, N., Dwiyanto, B., Parson, L. and Kallagher, H., 1992. The Manokwari trough and the western end of the New Guinea trench. *Tectonics*, 11: 145–153.
- Pacheco, J.F. and Sykes, L.R., 1992. Seismic moment catalog of large shallow earthquakes, 1900 to 1989. *Bull. Seismol. Soc. Am.*, 82: 1306–1349.
- Shimada, S. and Bock, Y., 1992. Crustal deformation measurements in central Japan determined by a global positioning system fixed-point network. *J. Geophys. Res.*, 97: 12,437–12,455.
- Stevens, C., McCaffrey, R., Bock, Y., Genrich, J., Calais, E., Wdowinski, S., Rais, J., Puntodewo, S.S.O., Subarya, C., Poewariardi, R., Brunner, F., Tregoning, P., Fauzi and Zwick, P., 1993. GPS measurements in Indonesia and preliminary results. *Eos Trans. AGU*, 74: 108.
- Thrupp, G.A., Sliter, W.V., Silver, E.A., Prasetyo, H. and Coe, R.S., 1987. Paleomagnetic evidence from Late Cretaceous rocks of Misool for rotation relative to Australia. *Eos, Trans. AGU*, 68: 1260.
- Weissel, J.K. and Anderson, R.N., 1978. Is there a Caroline plate? *Earth Planet. Sci. Lett.*, 41: 143–158.
- Visser, W.A. and Hermes, J.J., 1962. Geological results of the exploration for oil in the Netherlands New Guinea. *Verh. K. Ned. Geol. Mijnbouwkd. Genoot.*, 20: 1–265.